Orientation and layer thickness dependence on the longitudinal magnetization and transverse magnetization hysteresis loops of sputtered multilayer Fe/Si and Fe/Ge thin films

2004 J. Phys.: Condens. Matter 16 4121

(http://iopscience.iop.org/0953-8984/16/23/026)

INSTITUTE OF PHYSICS PUBLISHING JOURNAL OF PHYSICS: CONDENSED MATTER

J. Phys.: Condens. Matter **16** (2004) 4121–4129 PII: S0953-8984(04)76294-3

Orientation and layer thickness dependence on the longitudinal magnetization and transverse magnetization hysteresis loops of sputtered multilayer Fe/Si and Fe/Ge thin films

N A Morley[1], **M R J Gibbs**[1], **K Fronc**[2] **and R Zuberek**[2]

[1] Department of Physics and Astronomy, University of Sheffield, Sheffield S3 7RH, UK
[2] Institute of Physics, Polish Academy of Sciences, Aleja Lotnikow 32/56, 02-668 Warsaw, Poland

Received 22 January 2004
Published 28 May 2004
Online at stacks.iop.org/JPhysCM/16/4121
DOI: 10.1088/0953-8984/16/23/026

Abstract

The transverse magnetization and longitudinal magnetization hysteresis loops of sputtered thin films of Fe/Ge and Fe/Si multilayers on GaAs(001) substrates have been studied. The dependence of the film magnetic anisotropy on the bilayer period and semiconductor composition was investigated using a MOKE magnetometer. The hysteresis loops were measured as a function of the angle between the applied magnetic field and the hard–hard axis of the film. For the longitudinal magnetization, the Fe/Si film loops had lower remanent magnetization compared to the Fe/Ge film with the same spacer thickness. Thus the Fe/Si film had stronger exchange coupling across the spacer layer compared to the Fe/Ge film. For the thicker Ge spacer layer film, no exchange coupling was measured. For the transverse magnetization, the Fe/Ge multilayer films loops had only one Barkhausen jump. For the Fe/Si multilayer films loops, some contained one Barkhausen jump while others had two jumps, due to the cubic anisotropy contribution. These results are interpreted in terms of anisotropy and exchange energies.

1. Review of ultra-thin iron films

Over the last few years, great interest has been taken in the properties and structure of thin iron films grown on GaAs substrates. The films are either grown by molecular beam epitaxy (MBE) [1], or by dc sputtering [2–4]. For iron films fabricated by MBE, the magnetic [5, 6], electrical [7, 8] and structural [9–11] properties of the films have been studied. From these measurements, the anisotropy of the films was determined as a function of film thickness, such that for films thinner than 5 nm only uniaxial anisotropy occurred (see figure 1(a)). For films thicker than

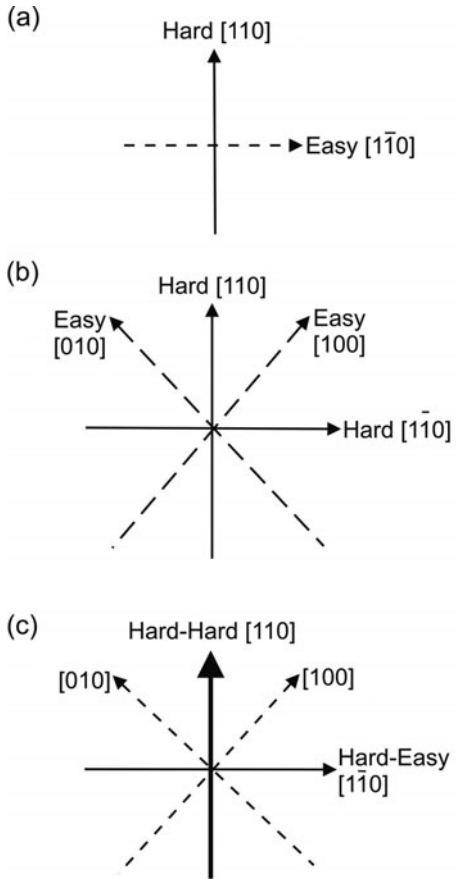

Figure 1. For a thin iron film the direction of the anisotropic energy axes, when the anisotropy is (a) uniaxial, (b) cubic, and (c) both. The easy axes are represented by the dashed lines and the hard axes are represented by the solid lines.

50 nm the anisotropy is cubic, reflecting the anisotropy of bulk iron (see figure 1(b)) [11, 12]. For film thicknesses between 5 and 50 nm the anisotropy is a combination of uniaxial and cubic (see figure 1(c)), with the easy axis of the uniaxial anisotropy along the same direction as a hard axis of the cubic anisotropy. The occurrence of the uniaxial anisotropy is thought to be due to the Fe–GaAs interface [13]; whether it is due to the presence of $Fe_3Ga_{2-x}As_x$ [14] or dangling bonds of GaAs [12] or the strain due to the lattice mismatch [15] is still not certain. Further investigations, to which this paper is a contribution, are being made which study the magnetostriction of these ultra-thin iron films.

As the magnetic anisotropy energy densities in the thin iron films are thickness dependent [16, 17], the total magnetic energy density changes as the thickness of the film increases. From figure 1(c), the hard axis of the uniaxial anisotropy is along one of the hard axes of the cubic anisotropy. Hence the total in-plane magnetic energy density of the film (F_{IPMA}), for no applied magnetic field, is given by

$$F_{\mathrm{IPMA}} = \tfrac{1}{4}K_1(t)\sin^2 2\varphi + K_{\mathrm{u}}(t)\sin^2(\varphi + 45) \tag{1}$$

where $K_1(t)$ is the cubic anisotropy constant, $K_{\mathrm{u}}(t)$ is the uniaxial anisotropy constant, and φ is the angle between the [100] direction and the in-plane magnetization. Both crystalline

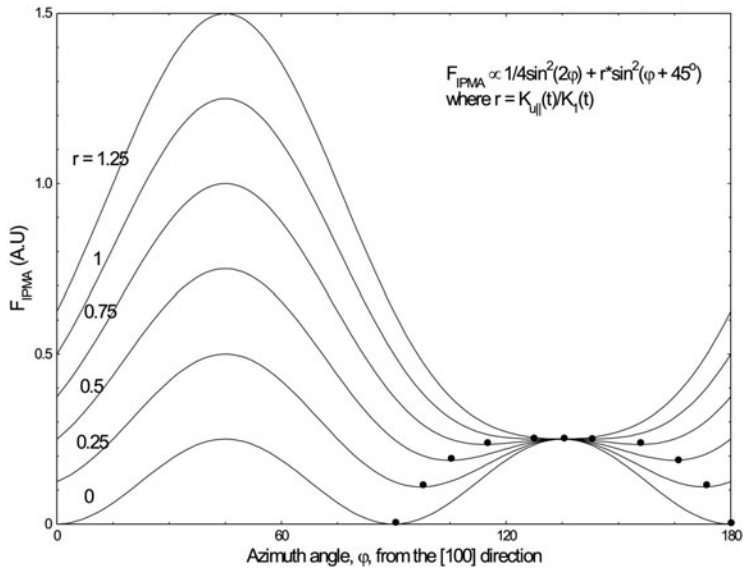

Figure 2. The total magnetic energy density for the in-plane magnetic anisotropy (IMPA) of a thin iron film, as a function of angle from the [100] direction and the ratio between the magnitude of the uniaxial ($K_{u\|}$) and cubic (K_1) anisotropy constants (r), when no magnetic field is applied. The two minima (the easy axes) for each loop are denoted by a dot.

anisotropy constants may be functions of the Fe layer thickness, t. The total magnetic energy density as a function of angle may be plotted using equation (1). From figure 2, it is seen that the angular positions and depth of the minima of the magnetic energy density move as the ratio $K_u(t)/K_1(t) = r$ decreases, i.e., as the thickness of the film increases. The behaviour of the magnetization in the iron films is dependent on the direction of the magnetic field to the [100] direction [5]. Hence if the applied magnetic field is not along one of the anisotropy energy easy axes, the magnetization will coherently rotate within the film from the field direction to the closest easy axes [1]. For magnetization by coherent moment rotation, the field at which the magnetization reaches saturation is known as the anisotropy field (H_A).

The films have two hard axes of different energy density (see figure 2), which means that the magnetization will rotate and jump over the hard axes so as to minimize the total energy density. This behaviour of the magnetization is observed in the transverse magnetization loops. The field can be applied at different angles to a crystallographic axis; a positive angle is taken in a clockwise direction from the axis. From Daboo *et al* [18], when the field is applied at an angle 30° to the [100] direction, the transverse magnetization loop has one Barkhausen jump, as the magnetization has jumped both the hard axes and the field at the same time. When the field is applied at an angle −65° to the [100] direction, then two Barkhausen jumps occur in the transverse magnetization loop. The magnetization coherently rotates to the closest easy axis, and then jumps the hard–easy axis, but not the hard–hard axis or the field direction. The magnetization then continues to rotate, before jumping the hard–hard axis and the field direction; thus two jumps appear in the hysteresis loop. When the field is applied at an angle 15° to the [100] direction, then again two Barkhausen jumps occur in the transverse magnetization loop. For this field direction, the magnetization coherently rotates away from the hard–easy axis, but then changes direction to jump over it, before rotating again and jumping over the hard–hard axis and the field. These jumps are less well defined in the longitudinal magnetization loops.

Multilayer films where the iron is layered with a non-magnetic material such as silicon have also been investigated [3, 19, 20]. The films show similar behaviour to single layer films, i.e., they have cubic and uniaxial anisotropy, but have an added exchange interaction across the non-magnetic spacer layer [4, 21]. The exchange coupling introduces another energy density into the total magnetic energy density of the iron film, which can either be bilinear [20, 22] or biquadratic [21]. Hence the total magnetic energy density of the film is given by [19]

$$F_{\mathrm{IPMA}} = \tfrac{1}{4}(K_{11}\sin^2 2\varphi_1 + K_{12}\sin^2 2\varphi_2) + K_{\mathrm{u}1}\sin^2(\varphi_1 - \theta_1) + K_{\mathrm{u}2}\sin^2(\varphi_2 - \theta_2) + \frac{1}{d}(I_1\cos(\varphi_1 - \varphi_2) + I_2\cos^2(\varphi_1 - \varphi_2)) - HM[\cos(\varphi_1 - \alpha) + \cos(\varphi_2 - \alpha)] \tag{2}$$

where d is the thickness of the film, I_1 and I_2 are the bilinear and biquadratic exchange constants, HM is the Zeeman energy, and subscripts 1 and 2 denote the upper and lower iron layers respectively. The angle φ_i is between the [100] direction and the magnetization, θ_i is the angle between the [100] direction and the hard axis for the layer i, and α is the angle between the [100] direction and the applied magnetic field. For the bilinear exchange ($I_1 > 0$), the coupling between the layers tends to be antiferromagnetic [23], which is taken to be the case at room temperature. For the biquadratic exchange ($I_2 > 0$), the interlayer coupling favours 90° alignment; this interaction is generally the stronger exchange at low temperatures [8]. The characteristic of the exchange interaction is a low remanent magnetization, in comparison to a single layer of iron [22]. These exchange interactions have been observed in Fe/Si/Fe trilayers but not in Fe/Ge/Fe trilayers [24]. The spacer layer between the two iron layers can cause the alignment of the anisotropy energy axes in each layer to be at a different angle to each other [21] and thus to the GaAs substrate layer.

This paper investigates multilayer Fe/semiconductor films on GaAs, to determine how the non-magnetic layer thickness and composition changes the overall crystalline anisotropy and exchange interactions. The data on Fe/Ge multilayers shows, for the first time, that there is bilinear coupling in this system for low Fe film thicknesses.

2. Experimental details

The three samples were fabricated using dc sputtering as described in the paper by Zuberek *et al* [25]. All three samples were grown on GaAs substrates on the (001) plane, such that the hard–hard axis was along the [110] direction, which was along one edge of the sample; hence the hard–easy axis was along the orthogonal edge. If the anisotropy was cubic then the two easy axes would lie along the [100] and [010] directions (see figure 1(b)). Due to the uniaxial anisotropy, the easy axes lay between these directions and the hard–easy axis (see figure 2). Each ultra-thin film was a single crystal as confirmed by x-ray analysis [26]. The thickness of each iron layer was 2.5 nm, for sample 1 the spacer layer was silicon of thickness 1.2 nm; the two layers were repeated 23 times, with a 7.5 nm silicon capping layer. For samples 2 and 3 the spacer layer was germanium, for sample 2 the thickness was 1.2 nm, and for sample 3 the thickness was 2.0 nm. For both samples the two layers were repeated 22 times, and finished with a 10 nm silicon capping layer.

The samples were measured on a transverse magneto-optic Kerr effect (MOKE) magnetometer at a laser wavelength of 633 nm. The angle of the polarizer was set such that the laser beam as incident on the sample was polarized to measure either the magnetization component parallel to the plane of incidence (longitudinal) or the magnetization component perpendicular to the plane of incidence (transverse). Hence for the longitudinal loops the polarizer was set at 51°, and for the transverse loops the polarizer was set at 90° [27]. An

analyser set at 2° from extinction was placed after the sample, followed by a photodetector, which measured the change in intensity of the laser. The voltage output of the photodetector was directly proportional to the normalized magnetization. The samples were measured in the centre of the electromagnet pole pieces, with the angle between the field and the hard–hard axis determined by reference to the edge of the sample.

3. Results

For each of the three samples, the transverse magnetization and longitudinal magnetization hysteresis loops were measured with the field along both hard axes, close to an easy axis, between the hard–hard axis and an easy axis, and between the hard–easy axis and an easy axis; for reference see figure 1. For each field direction, the field was swept from +350 to −350 mT and back again, with each loop containing 128 points. For the longitudinal magnetization loops, the photodetector voltage was amplified by 100, while for the transverse magnetization loops the voltage was amplified by 500. The longitudinal loops were normalized taking the saturation magnetization equal to ± 1. For each sample, all the transverse loops were normalized by the change in voltage of the hard–easy loop's transition.

For sample 1 (Fe/Si 1.2 nm) (see figure 3(a)), the longitudinal magnetization loops showed both the change in hysteresis due to the field being at different angles to the [100] direction, and the exchange interaction between the iron layers. The size of the Barkhausen jump in the hysteresis loop gives some indication of the direction of the field relative to the easy axis. The curvature on the loop for all directions apart from along the hard–hard axis can be interpreted directly in terms of equation (2) and the magnetic energy density model. For the transverse magnetization loops (see figure 3(b)), for the field directions between a hard axis and an easy axis, and close to an easy axis, only one Barkhausen jump appeared. Along the hard–hard axis no loop was measured while along the hard–easy axis, the loop contained two Barkhausen jumps for each field sweep.

For sample 2 (Fe/Ge 1.2 nm) (see figure 4(a)), the longitudinal loops had higher remanent magnetization than the same loops for sample 1; hence the exchange interaction was weaker between the iron layers. The hard axis loops were more curved and had smaller Barkhausen jumps than the easy axis loop; hence the film has cubic and uniaxial anisotropies. For the transverse loops (see figure 4(b)), only one Barkhausen jump was measured for any of the field directions. Along the hard–easy axis, the loop was almost circular, and contained no jumps.

For sample 3 (Fe/Ge 2 nm) (see figure 5(b)), the transverse hysteresis loops contained only one Barkhausen jump, including the loop for the field along the hard–easy axis, although it was almost circular. For the longitudinal loops the hard–hard axis loop had hysteresis, which was unexpected for this field direction (see figure 5(a)). Comparing the shape of the hard–easy axis loop to the easy axis loop, the film only contains uniaxial anisotropy, as the hard–easy axis loop has no moment rotation. Hence the hard–easy axis is the easy axis direction and the hard–hard axis is the hard axis direction (see figure 1).

4. Analysis and discussion

From measuring these three multilayer iron films, the exchange coupling and magnetocrystalline anisotropy as a function of spacer layer composition and thickness were investigated. It is not our intention here to directly extract the anisotropy constants from the data using equation (2), as the final normalized magnetization loop is a convolution of equation (2) with the magneto-optic response. This will be discussed in a later paper. Here the emphasis

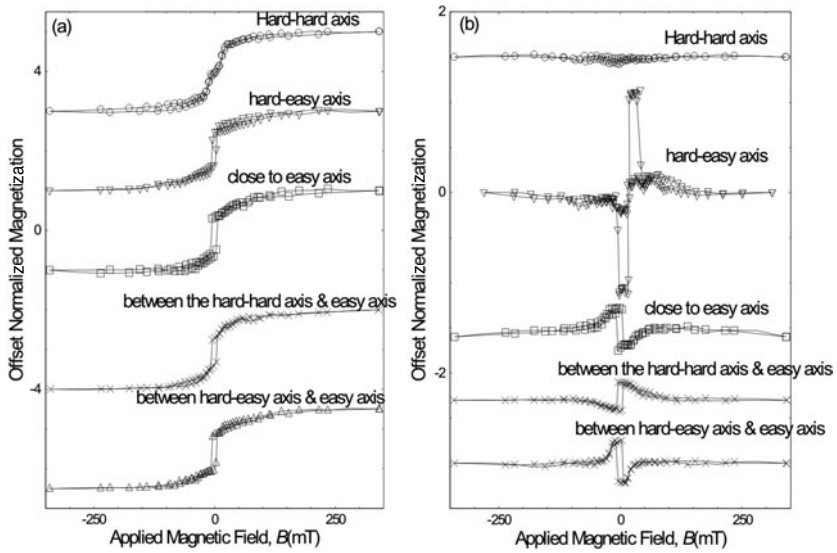

Figure 3. Normalized magnetization hysteresis loops for sample 1 [Fe(2.5 nm)/Si(1.2 nm)] as a function of applied magnetic field, for the field along different directions with respect to the anisotropy axes, for (a) the longitudinal magnetization, and (b) the transverse magnetization. The hysteresis loops are offset along the *y*-axis so the difference in their shapes is observed.

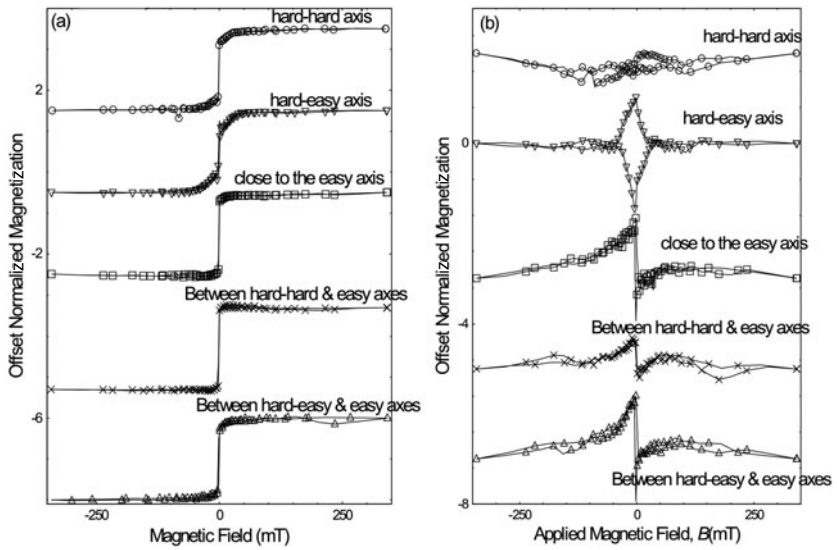

Figure 4. Normalized magnetization hysteresis loops for sample 2 [Fe(2.5 nm)/Ge(1.2 nm)] as a function of applied magnetic field, for the field along different directions with respect to the anisotropy axes, for (a) the longitudinal magnetization, and (b) the transverse magnetization. The hysteresis loops are offset along the *y*-axis so the difference in their shapes is observed.

is on the differences in magnetization behaviour for different spacer layers. For comparison between the different spacer layers, the magnetization hysteresis loops of samples 1 and 2 are compared. For sample 1, there was no magnetic saturation observed for fields up to 250 mT.

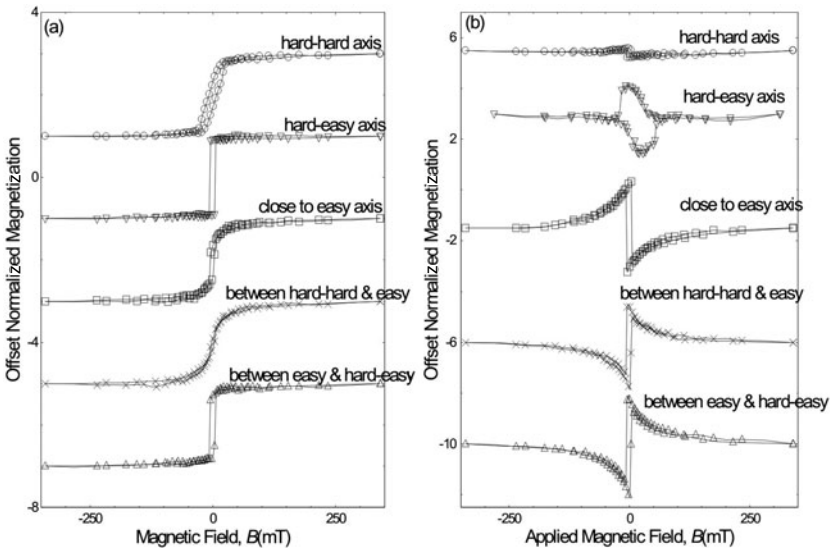

Figure 5. Normalized magnetization hysteresis loops for sample 3 [Fe(2.5 nm)/Ge(2 nm)] as a function of applied magnetic field, for the field along different directions with respect to the anisotropy axes, for (a) the longitudinal magnetization, and (b) the transverse magnetization. The hysteresis loops are offset along the y-axis so the difference in their shapes is observed.

The reasons for this could be that there was a strong exchange coupling between the iron layers, or the anisotropy energy axes in the different iron layers were not aligned with each other at zero field. However, for sample 2 (see figure 4(a)), the longitudinal loops have reached saturation magnetization in the fields applied, i.e., equivalent to the behaviour of a single layer film. The reasons for this could be that the anisotropy energy axes in adjacent iron layers were aligned at zero field or the exchange coupling across the Ge spacer layer was weak. The heights of the Barkhausen jumps for sample 1 were smaller than for sample 2, as the exchange interaction reduced the remanent magnetization [22]. In previous work, the exchange coupling has been observed across silicon spacer layers but not germanium layers [24]. For sample 2, the weaker exchange coupling across the germanium layer could be due to the germanium layer forcing the anisotropy energy axes of each layer to be in the same direction, or the iron layers were aligned ferromagnetically. From magnetoresistance measurements, to be published elsewhere, sample 2 does have weak exchange coupling between the iron layers [28].

For sample 1, the transverse magnetization loops contained two clear Barkhausen jumps when the field was aligned along the hard–easy axis, while for sample 2 the hard–easy axis loop contained two transitions, which were not Barkhausen jumps. This suggests that the Si spacer layers increased the cubic anisotropy in the iron layers, compared to the Ge spacer layers [29].

The thickness dependence of the non-magnetic layers on the properties of the thin films was also investigated. Other properties of magnetic films which change with magnetic film thickness are the magneto-optic constant and the index of refraction [30]; these also change the overall magnitude of the MOKE signal from the film [31]. No account has been taken of this as we are studying features such as Barkhausen events rather than absolute magnetization.

For sample 3, the Ge spacer layer was 0.8 nm thicker than for sample 2. As the skin depth of iron is a factor 10^3 smaller than germanium, and 10^5 times smaller than silicon, it is the Fe thickness that is the limiting factor. We believe that the MOKE will measure the same

number of iron layers in each multilayer film. The film magnetizations were also measured on a VSM in a maximum field of 20 mT. For sample 2, the saturation magnetization was 1.35×10^6 A m^{-1}, while for sample 3 the saturation magnetization was 1.45×10^6 A m^{-1}. Within the constraints of such low field data we have no evidence that the Fe magnetization is other than that for bulk. The values are lower than 2.10×10^6 A m^{-1} as more than 250 mT is required for saturation.

For sample 2, all the longitudinal loops had Barkhausen jumps, while the longitudinal loops measured along the hard–hard axis and between the hard–hard axis and the easy axis (see figure 5(a)) for sample 3 contained no Barkhausen jumps. Hence across the thinner Ge layer the exchange coupling was bilinear, while the thicker Ge layer was too great for bilinear coupling to occur, thus uniaxial anisotropy was measured.

From figures 3(b), 4(b) and 5(b), reversible coherent rotation is measured when the field is applied along directions between the hard–hard axis and the hard–easy axis, but not along these axes. For all three samples no coherent rotation was observed for the field along the hard–hard axis. However, for the hard–easy axis loops, rotation was observed, but the loops were not reversible; instead they were symmetric. The transverse loops are more sensitive to the direction of the field with respect to the [100] direction, φ. The field direction also dictates the direction in which the magnetization rotates towards an easy axis (see figure 2). The longitudinal magnetization loop shape is unaffected by the angle φ, while for the transverse magnetization loops, the direction in which the magnetization rotates is observed in the loops. For example, in figure 3(b), for the transverse loop taken between the hard–hard axis and the easy axis, the magnetization rotates away from the saturation magnetization in the opposite direction to the easy axis loop. Similar behaviour is observed in the transverse magnetization loops of sample 2 (see figure 4(b)) and sample 3 (see figure 5(b)). Hence the transverse magnetization is sensitive to the direction of the field with respect to the [100] direction.

5. Conclusions

For single crystal sputtered Fe/Si and Fe/Ge multilayer films, with semiconductor spacer thickness 1.2 nm, cubic and uniaxial anisotropy was observed in the longitudinal magnetization and transverse magnetization hysteresis loops. For the thicker Ge spacer layer only uniaxial anisotropy was measured. The difference between the two non-magnetic spacer layers was observed as a reduction in the remanent magnetization in the Fe/Si film's longitudinal loops compared to the Fe/Ge films' loops. The reduction was due to the iron layers either side of the silicon layer interacting via the bilinear exchange coupling; thus for the same thickness germanium layers, the exchange coupling was weaker. The Fe/Si transverse magnetization loop for the field along the hard–easy axis contained two Barkhausen jumps, while for all field directions the Fe/Ge loops contained one Barkhausen jump. Hence the silicon layer induced a larger cubic anisotropy into the film, compared to the same thickness germanium layer.

References

[1] Doi M *et al* 2002 *J. Magn. Magn. Mater.* **240** 407
[2] Zuberek R *et al* 2003 *J. Magn. Magn. Mater.* **260** 386
[3] Zuberek R *et al* 2001 *Mater. Sci. Forum* **373–376** 141
[4] Kohlhepp J T *et al* 1996 *J. Magn. Magn. Mater.* **156** 261
[5] Lepine B *et al* 1999 *J. Cryst. Growth* **201/202** 702
[6] Chye Y *et al* 2002 *Appl. Phys. Lett.* **80** 449
[7] Crisan V *et al* 2002 *J. Magn. Magn. Mater.* **240** 417
[8] Ueda Y *et al* 2002 *J. Magn. Magn. Mater.* **239** 45

[9] Moosbuhler R *et al* 2002 *J. Appl. Phys.* **91** 8757
[10] Xu Y B *et al* 1999 *J. Magn. Magn. Mater.* **198/199** 703
[11] Haugan H J *et al* 2002 *J. Magn. Magn. Mater.* **247** 296
[12] Gester M *et al* 1996 *J. Appl. Phys.* **80** 347
[13] Brockmann M *et al* 1999 *J. Magn. Magn. Mater.* **198/199** 384
[14] Filipe A *et al* 1996 *Appl. Phys. Lett.* **70** 129
[15] Sander D *et al* 1999 *J. Magn. Magn. Mater.* **200** 439
[16] Bensch F *et al* 2002 *J. Appl. Phys.* **91** 8754
[17] Moore T A *et al* 2001 *J. Appl. Phys.* **89** 7018
[18] Daboo C *et al* 1995 *Phys. Rev.* B **51** 15964
[19] Strijkers G J *et al* 2000 *Phys. Rev. Lett.* **84** 1812
[20] Chizhik A B *et al* 2002 *J. Low Temp. Phys.* **28** 639
[21] Fullerton E E *et al* 1996 *Phys. Rev.* B **53** 5112
[22] Chizhik A B *et al* 2002 *J. Phys.: Condens. Matter* **14** 8969
[23] Kohlhepp J T *et al* 1997 *J. Magn. Magn. Mater.* **165** 431
[24] de Vries J J *et al* 1997 *J. Magn. Magn. Mater.* **165** 435
[25] Zuberek R *et al* 2000 *Physica* B **284–288** 1237
[26] Zuberek R *et al* 2001 *Czech. J. Phys.* **52** A169
[27] Florczak J M *et al* 1990 *J. Appl. Phys.* **67** 7520
[28] Morley N A *et al* 2004 *J. Magn. Magn. Mater.* submitted
[29] Daboo C *et al* 1994 *J. Appl. Phys.* **76** 5586
[30] Judy J H *et al* 1968 *IEEE Trans. Magn.* **4** 401
[31] Florczak J M *et al* 1991 *Phys. Rev.* B **44** 9338